Experimental testing of a breakwater integrated U-OWC

João C. C. Henriques, Luís M. C. Gato and António F. O. Falcão

Abstract—**In 2003, Boccotti proposed a U-shaped oscillating water column (U-OWC) for integration into breakwaters. In this configuration, the inner water column is connected to the sea by a U-shaped channel with the opening facing upwards rather than sideways or downwards. This allows the length of the OWC to be increased (and the resonant frequency reduced) without placing the opening too deep in the water, where the wave energy is attenuated by the distance to the free surface. The lip distance - defined as the distance from the top of the front wall of the U-OWC to mean sea level - is one of the key parameters in the design of this type of wave energy converter. This paper reports on experiments with a 1:40 scale U-OWC in a wave flume under regular waves. In the tested configuration, the results show that the pneumatic power available to the turbine decreases as the ratio of wave amplitude to lip distance increases. In addition, the pneumatic capture width ratio also decreases as the lip distance decreases, demonstrating that both wave amplitude and tidal range have a non-negligible influence on the performance of a U-OWC.**

Index Terms—**Wave energy, Oscillating water column, Peak-to-average power ratio control, U-OWC.**

I. Introduction

A Fixed oscillating water column (OWC) is a hollow structure enclosing an air chamber open to the sea at its submerged part. Waves excite the water column and its movement alternately compresses and decompresses the enclosed air above the internal free surface, driving a self-rectifying air turbine [1]. The power take-off (PTO) of an OWC is basically the air turbine coupled by a shaft to an electrical generator connected to the grid by a back-to-back converter. Self-rectifying air turbines are used due to the alternating nature of the pressure fluctuations within the air chamber. Self-rectifying turbines avoid the aerodynamic losses associated with the rectifying valves required to use unidirectional turbines [2]. Two basic types of self-rectifying air turbines are used in OWCs: Wells turbines and impulse turbines [3]. The former have a linear relationship between pressure and flow up to hard stall conditions, while the latter have an almost quadratic relationship between pressure and flow.

This research was partially supported by the Portuguese Foundation for Science and Technology - FCT, through IDMEC, under LAETA, project UIDB/50022/2020.

J.C.C. Henriques, L.M.C. Gato, A.F.O. Falcão are with IDMEC, Instituto Superior Técnico, Universidade de Lisboa, Av. Rovisco Pais, 1049-001 Lisboa, Portugal (e-mails: joaochenriques@tecnico.ulisboa.pt, luis.gato@tecnico.ulisboa.pt, antonio.falcao@tecnico.ulisboa.pt).

Digital Object Identifier:
https://doi.org/10.36688/ewtec-2023-448

Most studies aimed at improving the efficiency of OWCs have focused on PTO control [4]. In 2003, Boccotti [5] proposed a different approach by adding a front wall to fixed OWCs to create a U-shaped oscillating water channel. This configuration extends the length of the OWC and reduces its resonant frequency to a value within the range of frequencies found in the ocean wave spectrum.

Scialò et al. [6] optimised the power take-off system of a U-OWC power plant to be integrated into the breakwater to be built at Rocella Jonica, Mediterranean Sea, Italy. The wave climate at this site is characterised by low-energy sea states with sporadic Mediterranean storms. These storms are mild compared to Atlantic storms, but account for a significant fraction of the total annual wave energy. Ref. [6] demonstrated the need to introduce relief valves to ensure safe operation in the more energetic sea states. The relief valves are an active device used to dissipate the excess pneumatic power available to the turbine. This requirement is particularly important in the case of the Wells turbine due to its runway characteristics.

The aim of this work is to experimentally evaluate the performance of a U-OWC WEC designed by Fox at al. [7] at different water depths. Preliminary experimental results show that the capture width ratio decreases significantly at lower water depths due to non-linear effects that were not considered during the design phase, which was based on linear wave theory. These non-linear effects open up the possibility of passive control of the pneumatic power peaks available to the air turbine. It should be emphasised that this approach only applies to low tide amplitude areas such as the Mediterranean.

Only the initial undisturbed waves have been considered in this study due to the large reflections in the flume. As air is a compressible fluid, the spring-like effect in the OWC chamber can affect the entire energy conversion chain in OWC converters. This spring-like compressibility effect has been known since the mid-1980s, but has been neglected in most experimental studies [8]. In this work, the air compressibility effects have been modelled by a proper scaling of the air chamber volume [1], [9].

The paper is divided into the following sections. Section 2 presents the design and construction of the model. Section 3 presents the experimental setup and methods, and Section 4 presents the experimental results and their discussion. Finally, section 5 summarises the conclusions.

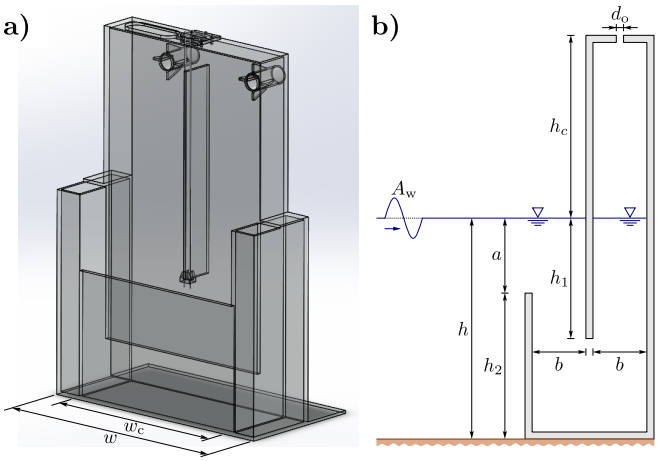

Fig. 1. Definition of the general dimensions of the U-OWC. a) Three-dimensional view and b) side view of the U-OWC model used in the experimental tests.

TABLE I
GENERAL DIMENSIONS OF THE U-OWC MODEL. *THE HEIGHT OF THE AIR CHAMBER AND THE EXTRA VOLUME FITTED TO THE MODEL WERE DETERMINED TO ACCURATELY SCALE THE EFFECTS OF AIR COMPRESSIBILITY.

Dimension	Prototype [m]	Model [m]
w	30.0	0.690
w_c	23.0	0.530
h	18.0	0.414
h_c	12.0	*
h_1	12.0	0.276
h_2	15.0	0.345
a	3.0	0.069
b	4.0	0.092
d_o	1.5	0.035

II. MODEL DESIGN

The U-OWC structure was designed in SolidWorks, which also helped to simulate the forces and pressures within the air chamber. The width of the U-OWC model was assumed to be 0.690 m to allow some clearance for later removal. This dimension was used to scale all other dimensions. The model was therefore built to a scale of

$$\epsilon = \frac{0.690}{30.0} \approx \frac{1}{43.5}. \tag{1}$$

Extruded acrylic was chosen for the construction of the models and to see the oscillating water column at work, because it is transparent and has a good strength/cost ratio. The assembly was done with acrylic glue when the joint had to be permanent, and with silicone glue when the piece had to be replaced after testing. The main dimensions of the prototype and the model are given in Table. I. Most of the model dimensions have been rounded to the nearest millimetre. However, certain dimensions have been rounded up to an even number to maintain the symmetry of the WEC. This is the case for the width of the OWC duct, which would be 0.529 m, but was increased to 0.530 m to avoid asymmetry and changes to other dimensions.

As shown in [1], [8], [9], to simulate the spring-like compressibility of the air in the chamber, the volume of the chamber model V_m is scaled as

$$V_\mathrm{m} = \delta^{-1}\epsilon^2 V_\mathrm{p}, \tag{2}$$

Fig. 2. Views of the U-OWC model installed at the IST wave flume. The blue barrels in the photos were used to simulate the effects of air compressibility.

where $\delta = \rho_\mathrm{m}/\rho_\mathrm{p}$ is the ratio of the density of the water in the channel to that of the seawater, and $V_\mathrm{p} = 1104\,\mathrm{m}^3$ is the volume of the prototype chamber. Here we have assumed $\delta = 1$. A finite element analysis of stresses and strains ensured that the model, barrels and connecting hoses did not deform more than 0.2 mm. This level of stiffness is essential to accurately simulate the effects of compressibility.

The height of the model, which has been modified to facilitate the replacement of turbine simulator apertures and the calibration of wave probes. To solve the problem of scaling the air chamber volume to simulate the effects of compressibility, two 217 litre oil drums were purchased to provide the additional air chamber. Two 0.044 m diameter holes were drilled symmetrically at the rear of the model to connect the barrels to the air chamber using rigid hoses, see Fig. 2.

III. WAVE FLUME

The experimental tests were carried out at the Hydraulics Laboratory of the Instituto Superior Técnico (LHIST). The wave flume is 20 m long, 0.7 m wide and limited to a maximum water depth of 0.5 m. It consists of a wave generating system facing the fixed U-OWC model on the opposite side, with parallel glass walls to allow visualisation of the free surface motion. The wave generation system consists of a piston wave maker operated by a hydraulic system. The piston control system is also equipped with an active absorption system to cancel the reflection of waves from the paddle.

The flume is equipped with three resistive wave gauges which allow the free surface height to be measured at several locations simultaneously. A fourth resistive wave probe was used to measure the internal free surface motion of the OWC. The air chamber pressure relative to the atmosphere was measured using a Honeywell pressure sensor with a range of 5 inch of H_2O. Analogue signals were acquired using a National Instruments USB-6210 multifunction DAQ device at a sampling rate of 100 Hz.

IV. EXPERIMENTAL CAMPAIGN AND DATA ANALYSIS

Three water depths and three regular wave heights were considered. Two turbine simulators were tested.

TABLE II
ORIFICE DIAMETERS, WATER DEPTHS AND WAVE HEIGHTS USED IN THE EXPERIMENTAL TESTS.

d_o [m]	h [m]	A_w [m]
0.035	0.441	0.0115
0.027	0.464	0.0345

TABLE III
SETS OF EXPERIMENTAL TESTS: LIP CLEARANCE TO DEPTH RATIOS a/h AND WAVE AMPLITUDE TO LIP CLEARANCE RATIOS A_w/a.

Test type	a/h	A_w/a
depth 1	0.218	0.120
		0.360
depth 2	0.256	0.097
		0.290

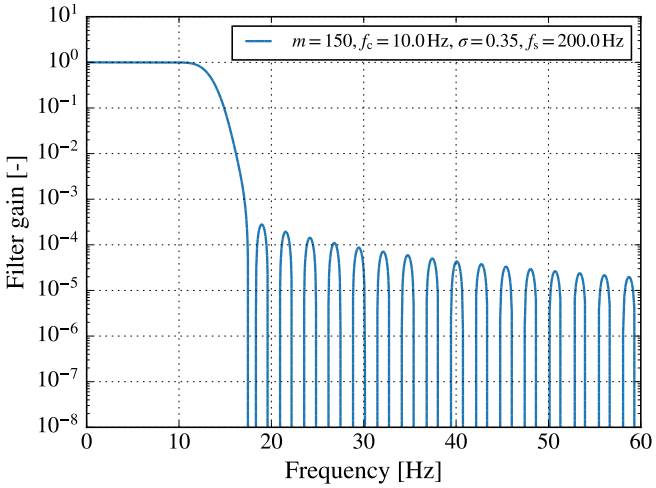

Fig. 3. Noise reduction filter gain as a function of the frequency.

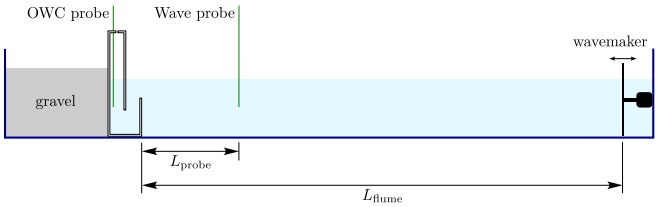

Fig. 4. Main dimensions of the wave flume and position of the wave and OWC probes.

The largest corresponds to the optimal diameter found in the U-OWC optimal design [7]. A smaller diameter orifice was also tested to assess the effect of turbine damping on the performance of the U-OWC. The tests performed considered all combinations of orifice diameters d_o, water depths h and wave heights H shown in Table. II. The following dimensionless parameters were defined to compare the different cases:

- Lip clearance to water depth ratio a/h, see Fig. 1.
- Wave amplitude to lip clearance ratio A_w/a.
- Orifice area to OWC free surface ratio S_o/S_c, where $S_o = \pi d_o^2/4$ and $S_c = w_c b$,

The dimensionless parameters related to water depth and wave height are presented in Tab. III. All tests shown in Tab. III were performed for the two orifice diameters corresponding to $S_o/S_c = 0.024$ and $S_o/S_c = 0.014$. The lower depth corresponds to the U-OWC optimum design condition reported in [7].

For the shallowest depth, a range of wave frequencies between 0.20 and 1.50 Hz was investigated. The values obtained were unsatisfactory in the range 0.20 to 0.48 Hz due to excessive uncertainty in the imposition of the wave height caused by the wavemaker controller. The frequency range was then reduced to wave frequencies between 0.50 and 1.50 Hz in steps of 0.02 Hz. Two further depths were investigated. The design depth was increased by 0.023 m and 0.046 m at model scale, corresponding to 1 m and 2 m at prototype scale. For these depths the frequency range was reduced from 0.50 to 1.20 Hz with a step of 0.02 Hz. A total of 792 frequency tests were performed with a typical duration of 80 s each. The mean value parameters evaluated during the experiments were (i) the OWC free surface response amplitude operator; (ii) the air chamber pressure response amplitude operator; (iii) and the capture width ratio.

Prior to all calculations, a noise reduction filter was applied to all time series. Air pressure relative to atmosphere was the noisiest signal. Filtering ensured that the average amplitude based on the peak-finding algorithm worked correctly. The used filter was a exponentially-windowed sinc filter defined as

$$\mathrm{f}[i] = \frac{1}{\nu}\mathrm{g}[i]. \tag{3}$$

with

$$\mathrm{g}[i] = \mathrm{sinc}(f_c i)\exp\left(-\frac{i^2}{2\sigma^2}\right), \tag{4}$$

where $i = -m, \ldots, 0, \ldots, m$ is the filter coefficient entry, ν is the normalisation factor given by

$$\nu = \sum_{k=-m}^{m} f[k], \tag{5}$$

f_c is the cutoff frequency, and σ is a parameter defining the window decay. The sinc function is defined as $\sin(\pi x)/(\pi x)$. The filter used in the present work is depicted in Fig. 3.

The response amplitude operator of the OWC free surface displacement y is defined

$$\mathrm{RAO}_y = \frac{\overline{A}_y}{\overline{A}_w}, \tag{6}$$

where $\overline{A}_y$ is the mean amplitude of the OWC free surface elevation with respect to the mean water level, and $\overline{A}_w$ is the mean wave amplitude.

The mean OWC free surface displacement amplitude is calculated from

$$\overline{A}_y = \frac{1}{2}\left(\overline{y}_{up} - \overline{y}_{lw}\right). \tag{7}$$

Here $\overline{y}_{up}$ is the mean of the upper peaks of y within the time interval $t \in [t_{y1}, t_{y2}]$. The lower limit t_{y1} is the initial signal disturbance instant t_{y0} plus 6 s of ramp up imposed by the wavemaker controller. The upper limit t_{y2} is given by

$$t_{y2} = t_{y0} + \frac{1.8 L_{flume}}{c_g}, \tag{8}$$

where L_{flume} is the distance from the wavemaker to the U-OWC front wall. We have used considered a

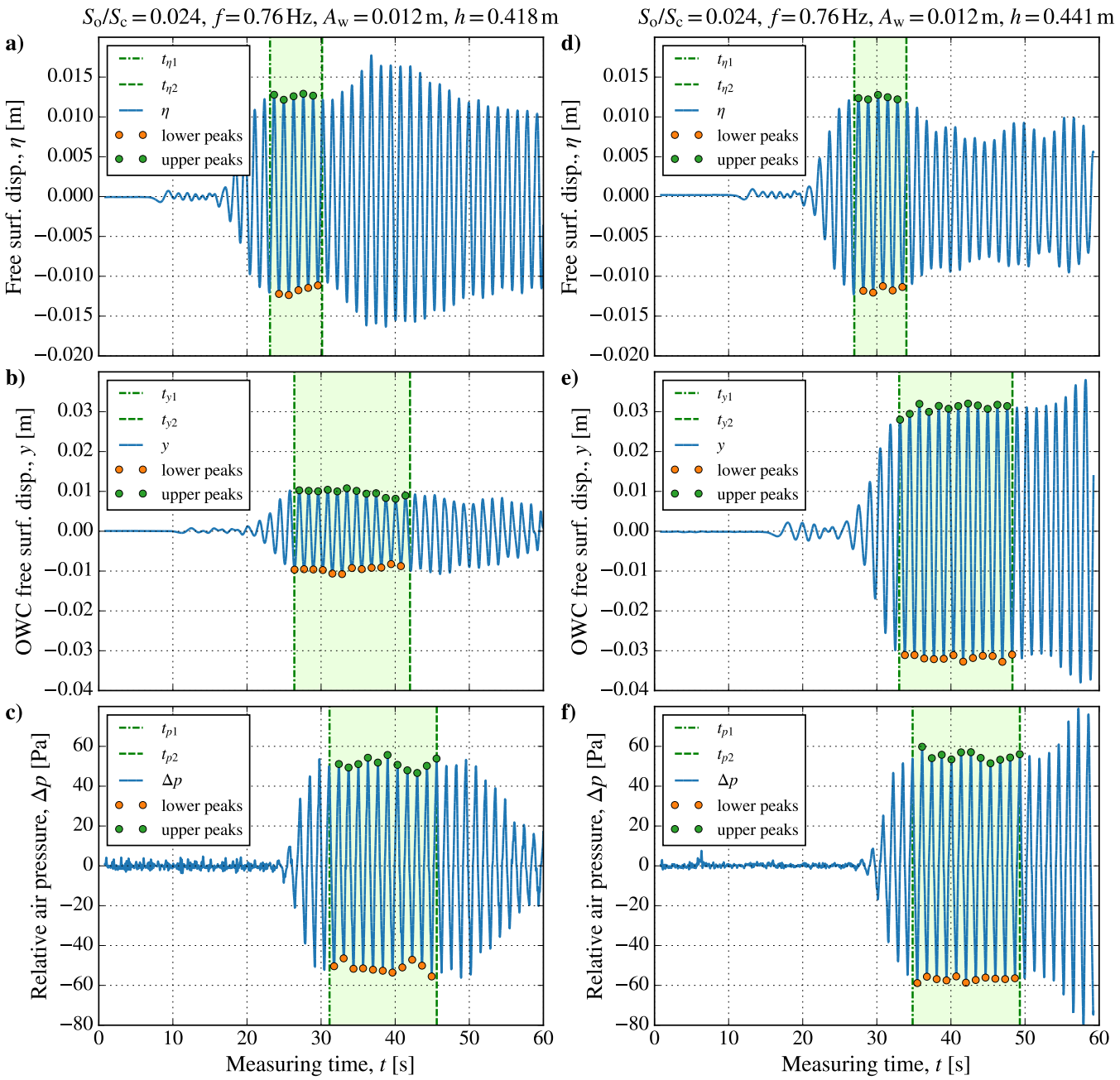

Fig. 5. a) Wave free surface displacement η, b) OWC free surface displacement η, and air chamber pressure Δp as a function of the measurement time t. Also show are the intervals limits used for the select the upper peak and lower peaks used the computation of the amplitudes.

travelling distance of $1.8L_{\text{flume}}$ instead of twice the flume length due to the uncertainty associated with the initial instant t_{y0}. This ensures that the y signal does not include waves reflected by the power plant. Similarly, $\overline{y}_{\text{lw}}$ is the mean of the lower peaks of y within the same time interval. Note that $\overline{y}_{\text{lw}} < 0$.

The mean wave amplitude η is computed as the mean OWC free surface displacement amplitude but considering a different time interval $t \in [t_{\eta 1}, t_{\eta 2}]$. The lower limit $t_{\eta 1}$ is again the initial signal disturbance instant $t_{\eta 0}$ plus the 6 s of ramp up, while the upper limit $t_{\eta 2}$ is given by

$$t_{\eta 2} = t_{\eta 0} + \frac{1.8 L_{\text{probe}}}{c_{\text{g}}}. \tag{9}$$

The group velocity is defined as

$$c_g = \frac{\omega}{2k}\left(1 + \frac{2kh}{\sinh(2kh)}\right). \tag{10}$$

The wavenumber k can be calculated iteratively using the well-known dispersion relation. In the present work we calculate the dimensionless wavenumber kh directly using You's approximation [10] defined by

$$kh = (k_0 h)\sqrt{1 + \left(k_0 h\left(1 + \sum_{n=1}^{5} D_n (k_0 h)^n\right)\right)^{-1}} \tag{11}$$

where $D_1 = 0.6522$, $D_2 = 0.4622$, $D_3 = 0$, $D_4 = 0.0864$, $D_5 = 0.0675$, $k_0 = \omega^2/g$, and ω is the angular frequency of the wave.

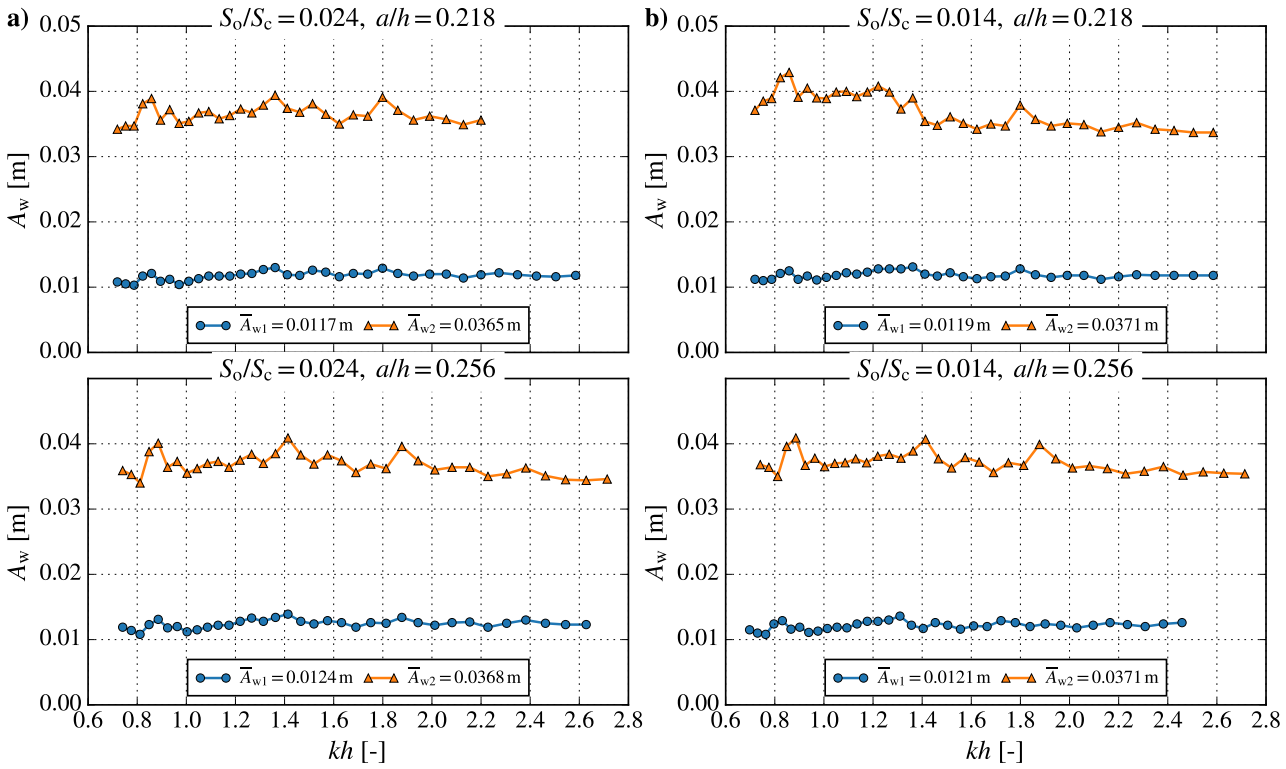

Fig. 6. Wave height as a function of the dimensionless wavenumber kh. Column a) presents the results for the larger orifice, while column b) is for the smaller orifice. The rows are in ascending order of water depth.

The response amplitude operator of the air chamber pressure is defined as

$$\mathrm{RAO}_{\Delta p} = \frac{\overline{\Delta p}}{\rho_\mathrm{w} g \overline{A}_\mathrm{w}}, \tag{12}$$

where $\overline{\Delta p}$ is the amplitude of the air chamber pressure relative to the atmosphere, ρ_w is the water density and g is the acceleration due to gravity. The definition of $\mathrm{RAO}_{\Delta p}$ is dimensionless. The amplitude of the air chamber pressure relative to the atmosphere is calculated as the mean OWC free surface displacement amplitude.

The pneumatic capture width ratio is defined as

$$\mathrm{CWR} = \frac{\overline{P}_\mathrm{pneu}}{\overline{P}_\mathrm{wave} w_\mathrm{c}}, \tag{13}$$

where $\overline{P}_\mathrm{pneu}$ is the mean pneumatic power and $\overline{P}_\mathrm{wave}$ is the mean wave power per unit wave crest. The average pneumatic power is calculated as

$$\overline{P}_\mathrm{pneu} = \frac{1}{t_{p2} - t_{p1}} \int_{t_{p1}}^{t_{p2}} Q \Delta p \, \mathrm{d}t. \tag{14}$$

The lower limit is equal to $t_{p1} = t_{p0} + 6\,\mathrm{s}$, where t_{p0} is the initial pressure perturbation instant, while the upper limit is determined to guarantee a time interval which is a multiple of the wave period T_w, thus giving

$$t_{p2} = t_{p1} + \mathrm{floor}\left(\frac{t_{p2} - t_{p1}}{T_\mathrm{w}}\right) T_\mathrm{w}. \tag{15}$$

Here the floor function of a real number x returns the greatest integer less than or equal to x. The flow rate Q through the orifice was correlated to the relative pressure Δp by

$$Q = \mathrm{sign}(\Delta p)\, S_\mathrm{o} C_\mathrm{d} \sqrt{\frac{2|\Delta p|}{\rho_\mathrm{air}}}, \tag{16}$$

where $C_\mathrm{d} = 0.66$ is the discharge coefficient calibrated experimentally, ρ_air is the atmospheric air density, and

$$\mathrm{sign}(x) = \begin{cases} +1, & \text{if } x > 0, \\ 0, & \text{if } x = 0, \\ -1, & \text{if } x < 0. \end{cases} \tag{17}$$

The mean wave power per unit wave crest is computed as

$$\overline{P}_\mathrm{wave} = \overline{E}\, c_g, \tag{18}$$

where

$$\overline{E} = \frac{1}{2} \rho_\mathrm{w} g A_\mathrm{w}^2. \tag{19}$$

V. Results

The Wavemaker controller installed in the flume used in the tests did not guarantee the prescribed wave amplitude. Therefore, in all the tests considered, it was necessary to fine-tune the prescribed wave amplitude to achieve a relatively small deviation from the mean amplitude. The fine-tuning has to be done by trial and error, as no pattern was found as a function of frequency. Figure 6 plots the obtained mean wave amplitude as a function of frequency for all tests performed. This shows that there are more deviations from the mean as the wave amplitude increases.

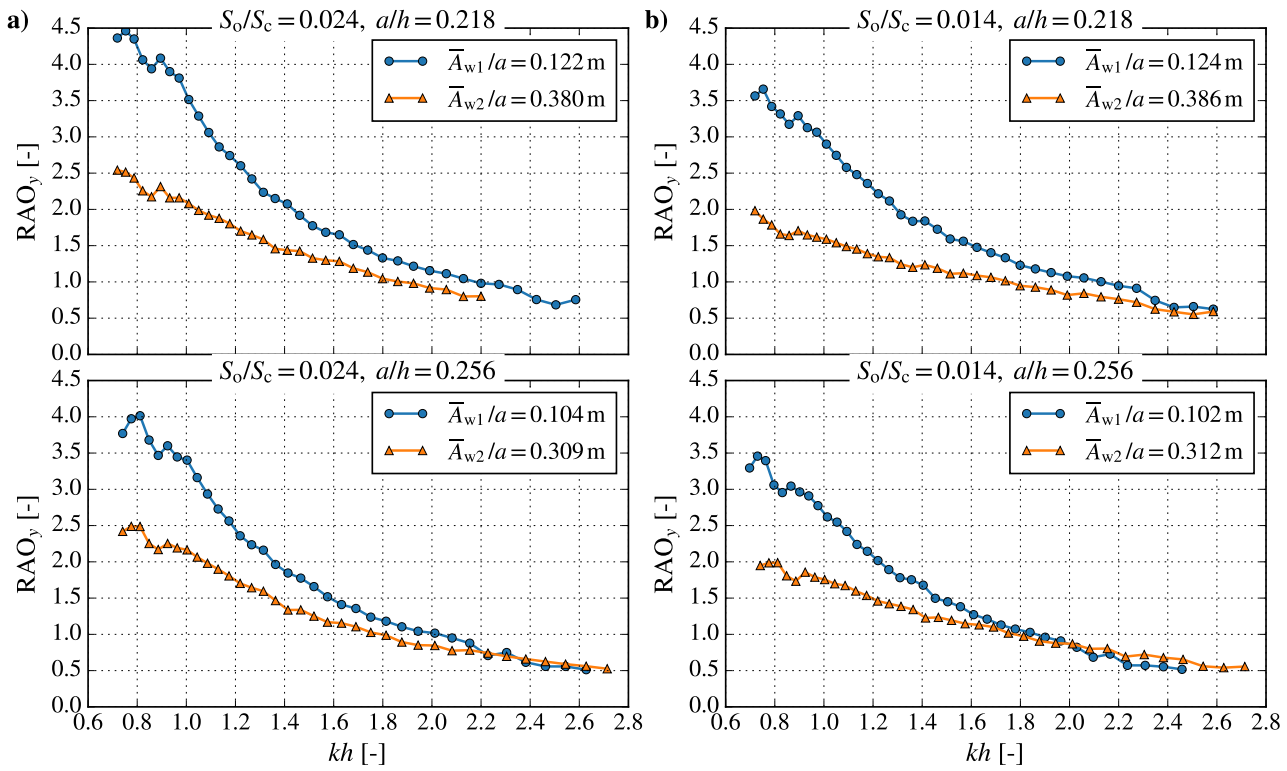

Fig. 7. Response amplitude operator of the OWC free surface displacement amplitude as a function of the dimensionless wavenumber kh. Column a) presents the results for the larger orifice, while column b) is for the smaller orifice. The rows are in ascending order of water depth.

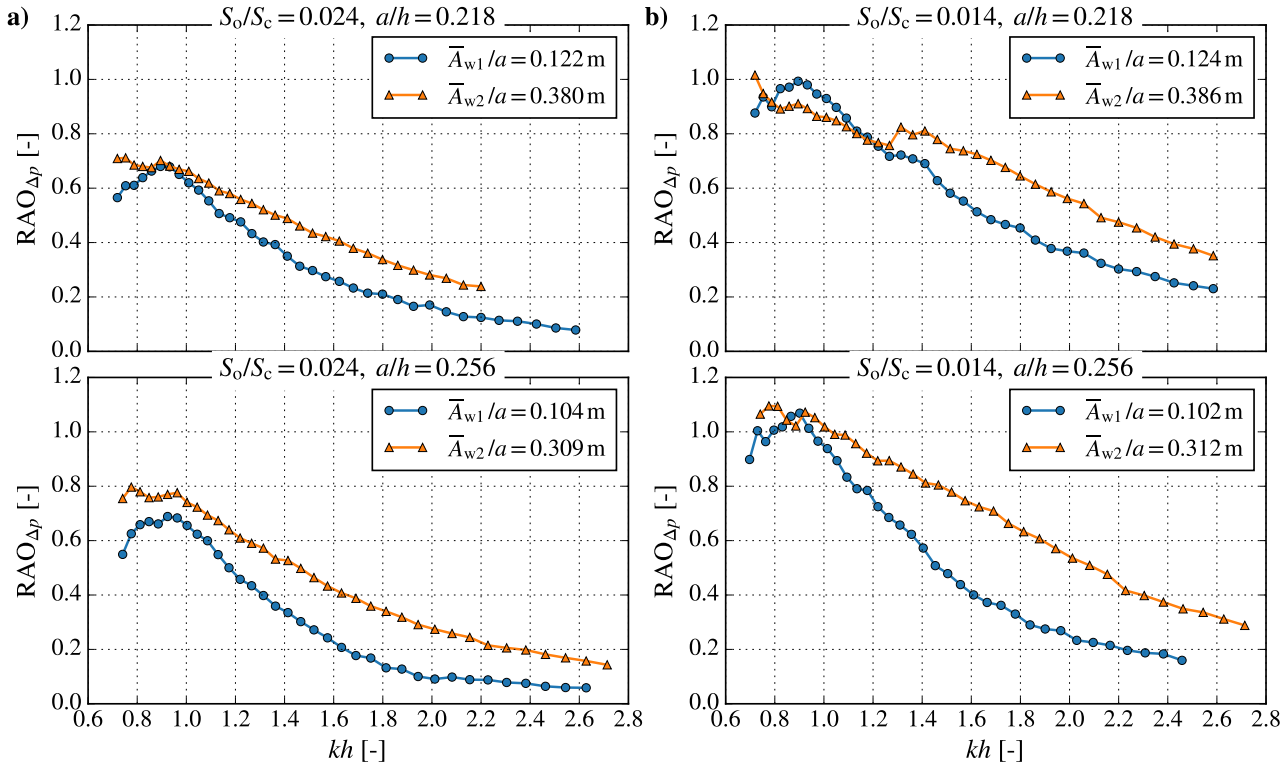

Fig. 8. Response amplitude operator for the OWC air chamber pressure relative to the atmosphere as a function of the dimensionless wavenumber kh. Column a) presents the results for the larger orifice, while column b) is for the smaller orifice. The rows are in ascending order of water depth.

The RAO_y, the $\mathrm{RAO}_{\Delta p}$ and the CWR results as a function of the dimensionless wavenumber kh, S_o/S_c, a/h and $\overline{A_w}/a$ are plotted in Figs. 7, 8 and 9 respectively. In all cases the general trends are independent of the orifice diameter, i.e. S_o/S_c. For all other depths, the results show that the RAO_y increases with decreasing $\overline{A_w}/a$. The $\mathrm{RAO}_{\Delta p}$ increases with depth for the same wave height. In general, the $\mathrm{RAO}_{\Delta p}$ increases

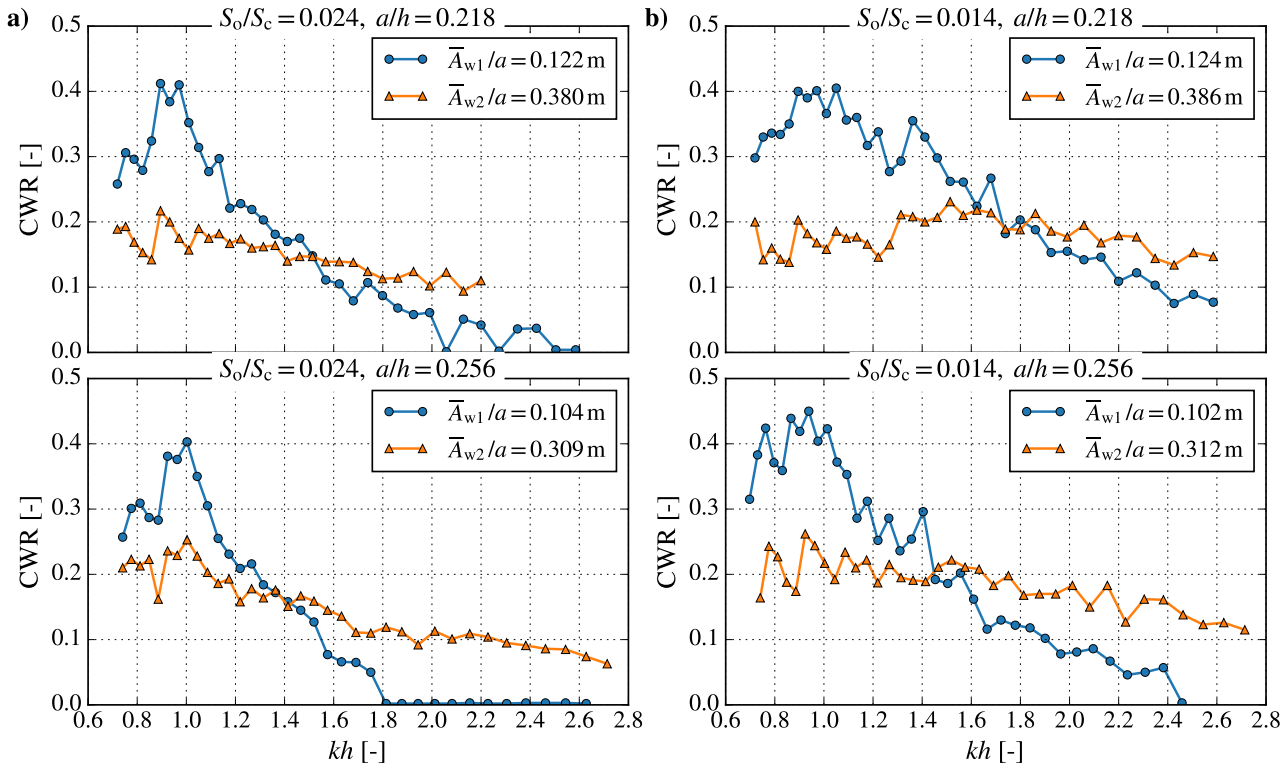

Fig. 9. Capture width ratio as a function of the frequency f. Column a) presents the results for the larger orifice, while column b) is for the smaller orifice. The rows are in ascending order of water depth.

with wave height for the highest frequencies, but the difference between the highest wave amplitudes and the medium amplitude waves is less than the difference between the medium waves and the lowest waves. The CWR is lowest at the shallowest depth. For the two depths considered, there is a range of lower frequencies where the CWR is higher for the smallest wave amplitude and a frequency where this behaviour changes, i.e. a range of high frequencies where the CWR is higher for the largest waves. This suggests that this is an effect of air compressibility. The capture width ratio is higher for the smallest orifice. This shows that the optimum turbine damping calculated by [7] using linear wave theory needs to be tuned experimentally.

VI. Conclusions

The paper reports an experimental evaluation of the performance of a breakwater-integrated U-OWC in a wave channel. The power plant was assumed to operate with an impulse turbine. The pneumatic damping of the turbine was therefore simulated using an orifice. The tests were carried out for two depths and two orifice diameters. The results showed that the U-OWC had a better CWR at low frequencies for all test conditions. In general, the CWR decreases as the wave height increases. This shows that it should be possible to find an optimum lip clearance for the U-OWC that allows the device to operate at maximum CWR at low to medium wave heights and reduces its efficiency as the wave height increases. The maximum power was verified for the smallest orifice for all conditions studied, although there was no significant difference. This shows that the optimum turbine damping needs to be tuned experimentally.

References

[1] A. F. O. Falcão and J. C. C. Henriques, "Oscillating-water-column wave energy converters and air turbines: A review," *Renewable Energy*, vol. 85, pp. 1391–1424, 2016.

[2] P. Benreguig, V. Pakrashi, and J. Murphy, "Assessment of primary energy conversion of a closed-circuit owc wave energy converter," *Energies*, vol. 12, no. 10, 2019.

[3] A. F. O. Falcão, J. C. C. Henriques, and L. M. C. Gato, "Self-rectifying air turbines for wave energy conversion: A comparative analysis," *Renewable and Sustainable Energy Reviews*, vol. 91, pp. 1231–1241, 2018.

[4] M. Rosati, J. C. C. Henriques, and J. V. Ringwood, "Oscillating-water-column wave energy converters: A critical review of numerical modelling and control," *Energy Conversion and Management: X*, vol. 16, p. 100322, 2022.

[5] P. Boccotti, "On a new wave energy absorber," *Ocean Engineering*, vol. 30, no. 9, pp. 1191–1200, 2003.

[6] A. Scialò, J. C. C. Henriques, G. Malara, A. F. O. Falcão, L. M. C. Gato, and F. Arena, "Power take-off selection for a fixed U-OWC wave power plant in the Mediterranean Sea: The case of Roccella Jonica," *Energy*, vol. 215, p. 119085, 2021.

[7] B. N. Fox, R. P. F. Gomes, and L. M. C. Gato, "Analysis of oscillating-water-column wave energy converter configurations for integration into caisson breakwaters," *Applied Energy*, vol. 295, p. 117023, 2021.

[8] A. F. O. Falcão and J. C. C. Henriques, "The spring-like air compressibility effect in oscillating-water-column wave energy converters: Review and analyses," *Renewable and Sustainable Energy Reviews*, vol. 112, pp. 483–498, 2019.

[9] J. C. C. Portillo, J. C. C. Henriques, L. M. C. Gato, and A. F. O. Falcão, "Model tests on a floating coaxial-duct owc wave energy converter with focus on the spring-like air compressibility effect," *Energy*, vol. 263, p. 125549, 2023.

[10] Z.-J. You, "A close approximation of wave dispersion relation for direct calculation of wavelength in any coastal water depth," *Applied Ocean Research*, vol. 30, no. 2, pp. 113–119, 2008.